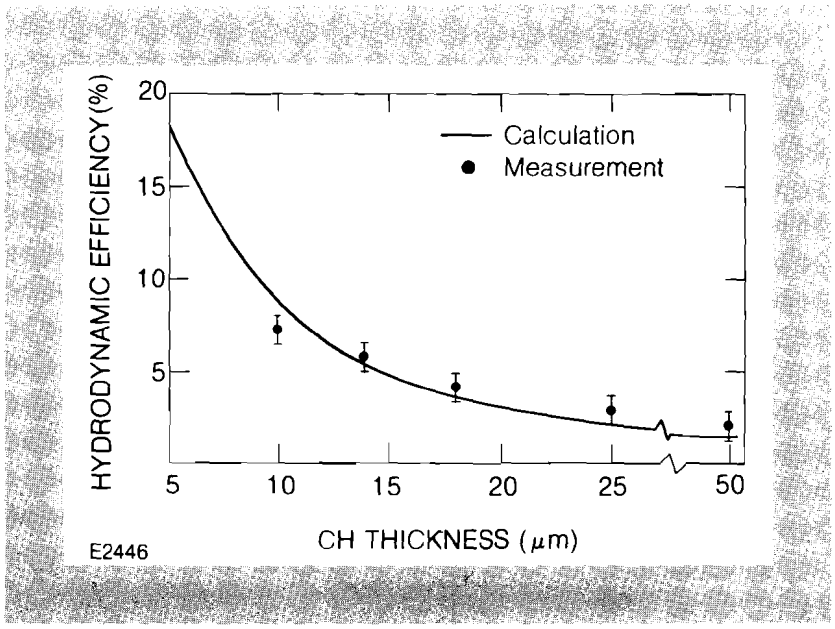

Fig. 9
Dependence of hydrodynamic efficiency on the thickness of CH targets for a constant intensity of 7.2×10^{13} W/cm^2 and a pulse width of 1 ns.

7.2×10^{13} W/cm^2). Again the agreement between the measured and the calculated values is close.

The major conclusion to be drawn from these experiments is that finite size targets may be used for hydrodynamic-efficiency measurements provided one properly takes into account the two-dimensional properties of the accelerated expansion.

REFERENCES

1. R. S. Craxton and R. L. McCrory, Laboratory for Laser Energetics Report No. 99 (1980); R. S. Craxton and R. L. McCrory, Laboratory for Laser Energetics Report No. 108 (1980).
2. W. Seka, R. S. Craxton, J. Delettrez, L. Goldman, R. Keck, R. L. McCrory, D. Shvarts, J. M. Soures, and R. Boni, *Opt. Commun.* **40**, 437 (1982).

2.C Theory of the Two-Plasmon Decay Instability in a Filament

Discrepancies between predictions of the conventional model of the two-plasmon decay and experimental observations of $3\omega_0/2$ spectra have led to consideration of a new model, where the decay occurs inside a filament. Predictions of the new model agree well with observations.

Of the various parametric instabilities which can be generated by laser light propagating through the corona, the two-plasmon decay instability (TPD) is one of the most difficult to diagnose. This problem arises because in TPD an incident photon decays into two plasma waves (plasmons) which are confined to the plasma, and thus cannot

be directly observed. The occurrence of the decay may be inferred from Thompson-scattering of a probe laser beam from the decay plasmon;[1] however, the simplest experimental signature is the generation of half-integer harmonic light at frequencies $\omega_0/2$, $3\omega_0/2$, etc. (where ω_0 is the frequency of the laser) by interaction of the decay plasmons with incident laser photons. The generation of the 3/2 harmonic is the easiest to understand, since it simply involves the "addition" of a plasmon of frequency $\sim \omega_0/2$ and a laser photon of frequency ω_0. The generation of $\omega_0/2$ light is more complicated, since it is produced not only by "subtraction" of a plasmon from an incident photon, but also by linear conversion of the decay plasmons to photons and by absolute Raman scattering.

The dispersion relation for plasma waves may be written

$$\omega^2 = \omega_p^2 [1 + 3 (k\lambda_D)^2] \tag{1}$$

where ω, k are the plasmon frequency and wave vector, respectively, ω_p is the local plasma frequency, and λ_D is the Debye length. Landau damping of short-wavelength plasmons imposes the restriction $k\lambda_D \lesssim 0.2$, so Eq. (1) implies that $\omega^2 \simeq \omega_p^2$. Thus, both plasmons in TPD must have frequencies approximately equal to ω_p. Since the sum of the two frequencies must equal ω_0, we see that the decay occurs for $\omega_p \simeq \omega_0/2$, or where the density is one-quarter of critical density.

TPD has usually been thought to occur at the quarter-critical surface of the bulk plasma density profile. To first approximation, this surface may be regarded as a plane perpendicular to the wave vector $\mathbf{k}_0$ of the incident light. The sum of the wave vectors of the two TPD plasmons must equal $\mathbf{k}_0$, and so they must have equal and opposite values of $\mathbf{k}_\perp$, the component of $\mathbf{k}$ perpendicular to $\mathbf{k}_0$. The sum of the frequencies of the two plasmons must equal ω_0, and so one has frequency $\omega_0/2 + \Delta$ and the other $\omega_0/2 - \Delta$. As explained in Ref. 2, the modes with maximum growth rate are determined by a hyperbola in $\mathbf{k}$-space; for these modes Δ is a function only of $|\mathbf{k}_\perp|$. When one of these plasmons is added to a laser photon to produce a $3\omega_0/2$ photon, the entire perpendicular component of the $3\omega_0/2$ photon wave vector must come from the plasmon: $(\mathbf{k}_{3/2})_\perp = (\mathbf{k})_\perp$. Since the density gradient is parallel to $\mathbf{k}_0$, $\mathbf{k}_\perp$ is conserved in the propagation of plasmons and photons, and it is this $\mathbf{k}_\perp$ which determines the angle θ at which the $3\omega_0/2$ photon is observed:

$$\sin\theta = \frac{1}{\sqrt{3}} \left| \frac{\mathbf{k}_\perp}{\mathbf{k}_0} \right|.$$

The spectral splitting Δ for these modes is

$$\Delta = \frac{3v_T^2 k_0^2}{2\omega_0} \sqrt{1 + 12 \sin^2\theta}. \tag{2}$$

Thus, at a given angle of observation θ, we expect to see two peaks in the $3\omega_0/2$ spectrum, shifted symmetrically by $\pm\Delta$ from the exact $3\omega_0/2$ frequency. This is consistent with experimental data at 1054-

nm; however, in experiments performed with 351-nm laser light the two peaks are always shifted asymmetrically, with the red shift two to three times larger than the blue shift. The strong angular dependence of the shift, predicted by Eq. (2), is not seen; the splitting is essentially independent of the angle of observation.

To explain these observations, a new model has been developed as shown in Fig. 10. We assume that, due to self-focusing, hot spots in the incident beam form small cylindrical channels in the plasma ("filaments") in which the central density is much lower than the background density n_0 outside the filament. If n_0 is larger than one-fourth of critical density, a cylindrical quarter-critical surface can be formed inside the filament, at which TPD can occur. For a linearly polarized pump, there exist regions of both s- and p-polarization in the filament, as shown.

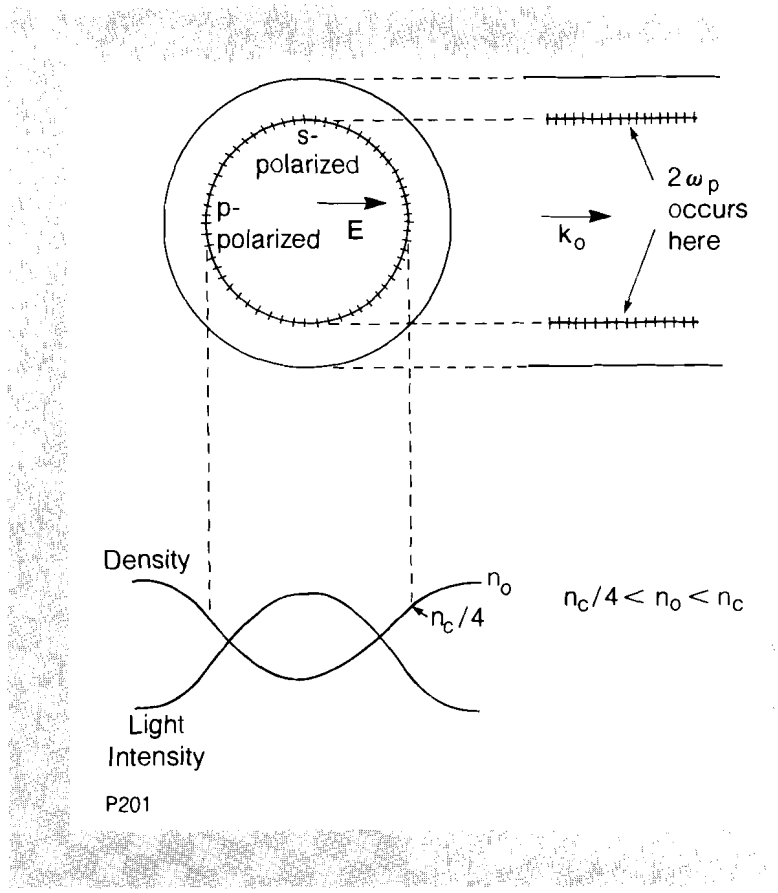

Fig. 10
Geometry of filament and quarter-critical surface. The hash marks show the quarter-critical region where two-plasmon decay occurs. The background plasma density is n_0, the wave vector of the light in the filament is $\mathbf{k}_0$, and n_c is the critical density.

To calculate approximate thresholds and growth rates for TPD in a filament, we use a simplified model, where we neglect the curvature of the filament wall (which should be valid for filament radii much larger than a wavelength) and the radial variation of the laser-light intensity (which is small over the region near quarter-critical where TPD is localized.) We first determine modes of the homogeneous problem which are absolute in the directions perpendicular to $\mathbf{k}_0$, so that they do not propagate away from quarter-critical density. These modes are determined by a hyperbola in **k**-space, as shown in Fig. 11, and also happen to be the modes with the largest growth rate.[2] The parameter κ

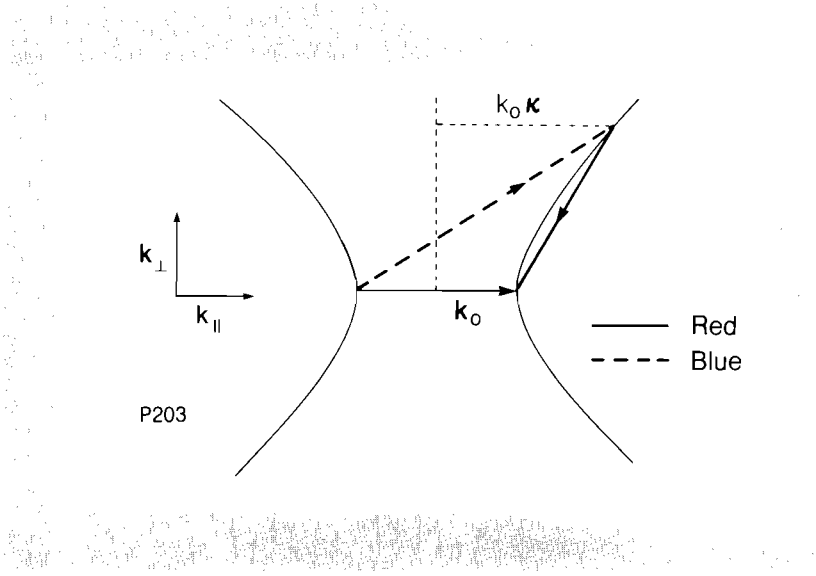

Fig. 11
Modes in homogeneous plasma which are non-propagating in directions perpendicular to the incident light wave vector k_0. Each point on the hyperbola represents the apex of a decay triangle, with the two-plasmon wave vectors adding to give k_0. The plasmon frequency shifts from the exact half-harmonic are proportional to the parameter κ, which is defined as the distance from a line bisecting k_0 to the apex of the decay triangle measured in units of k_0.

determines the frequency shift of the two plasmons from $\omega_0/2$; κ is 1/2 at the tip of the hyperbola and increases with larger wave vector plasmons. The effect of the radial density inhomogeneity may be obtained through a perturbation approach based on a WKB analysis of the Fourier-transformed plasma-wave equations[3]; the resulting frequencies are

$$\frac{\omega}{\omega_0} = \frac{1}{2} \pm 3\,\frac{v_T^2 k_0^2}{\omega_0^2}\,\kappa + i\frac{2}{3}\,\frac{k_0 v_0}{\omega_0}\left(1 - \frac{1}{\alpha\kappa}\right) \qquad \text{p-polarized}$$

$$\frac{\omega}{\omega_0} = \frac{1}{2} \pm 3\,\frac{v_T^2 k_0^2}{\omega_0^2}\,\kappa + i\frac{2}{3}\,\frac{k_0 v_0}{\omega_0}\left(1 - \frac{1}{\alpha\sqrt{\kappa^2 - 1/4}}\right) \qquad \text{s-polarized}$$

where $\alpha \equiv 4(k_0 v_0/\omega_0)k_0 L$, v_0 is the electron quiver velocity in the laser field, v_T is the electron thermal velocity, and L is the radial-density scale length. The second term on the right is the frequency shift, proportional to κ, and the last term is the growth rate. Instablity requires $\alpha\kappa > 1$; by choosing modes with **k** (and therefore κ) large enough this condition can always be satisfied. However, Landau damping limits the size of **k**, requiring $k\lambda_D \lesssim 0.2$. This yields a threshold condition:

$$\frac{v_0}{v_T} k_0 L > 3$$

In a filament we expect the ponderomotive force to essentially balance the thermal pressure force, and so we have $v_0/v_T \sim 1$. Also, the radial-density scale length should be one wavelength or longer, and so $k_0 L \sim 2\pi L/\lambda_0 \lesssim 2\pi$. Thus, the condition (Eq. 3) for TPD in a filament is readily satisfied.

In Fig. 12 we illustrate how the red-shifted $3\omega_0/2$ component is produced in a filament. A red-shifted plasmon propagates in the radial density profile until its wave vector is appropriate to add to $\mathbf{k}_0$ to produce the wave vector of a $3\omega_0/2$ photon. To produce this light in

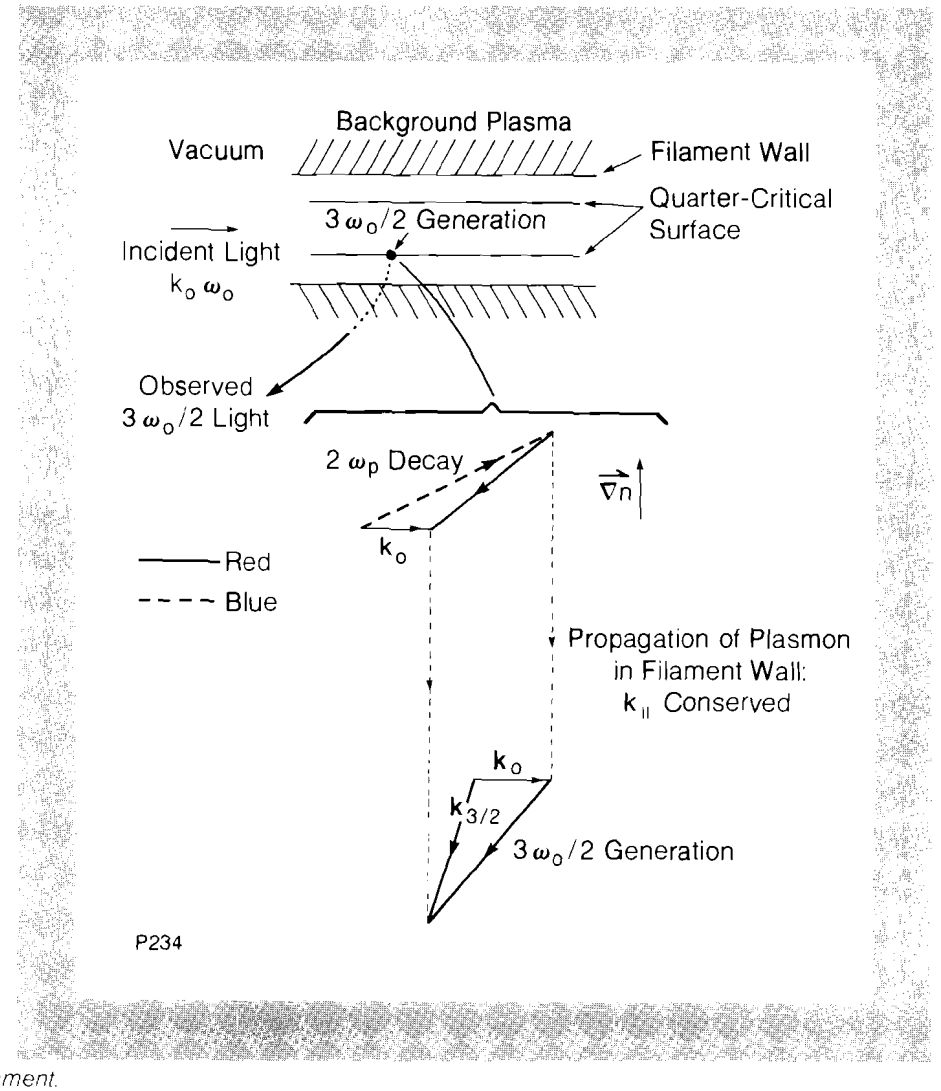

Fig. 12
Generation of 3/2-harmonic in a filament. The blow-up shows **k***-matching conditions for the generation of red-shifted backscattered 3/2-harmonic, as explained in text. The vector* ∇n *represents the radial-density gradient; the axial component of the plasmon wave vector,* $\mathbf{k}_{\parallel}$*, is conserved as the plasmon propagates in the filament.*

the backward direction, as shown here, **k** must be fairly long in order to cancel the forward-directed $\mathbf{k}_0$. Thus, these decays have large κ's and large red shifts. Red plasmons from decays with smaller κ's, and, thus, smaller red shifts, produce a red $3\omega_0/2$ peak in a range of angles in the forward direction, as shown in Fig. 13a. However, since $k_{3/2} > k_0$, $k_{3/2}$ must have a significant perpendicular component, and, thus, red-shifted $3\omega_0/2$ light is excluded from a cone angle of about 20° around the forward direction.

In Fig. 13b, we see the generation of blue-shifted $3\omega_0/2$ radiation. Since the blue plasmon has a $k_{\parallel}$ greater than k_0, the requirement that the sum of the blue plasmon and photon wave vectors yield a $3\omega_0/2$ wave vector means we must have $2k_0 < k_{3/2}$. Now $\mathbf{k}_0$ is the photon wave vector inside the filament, and its exact value depends on the detailed radial-density profile of the filament. However, $\mathbf{k}_0$ becomes smaller as the background density n_0 outside the filament becomes larger (larger background densities decrease the filament radius and increase the average radial density, both of which tend to decrease $\mathbf{k}_0$). If we take $\mathbf{k}_0$ to be the wave vector of laser light in the background

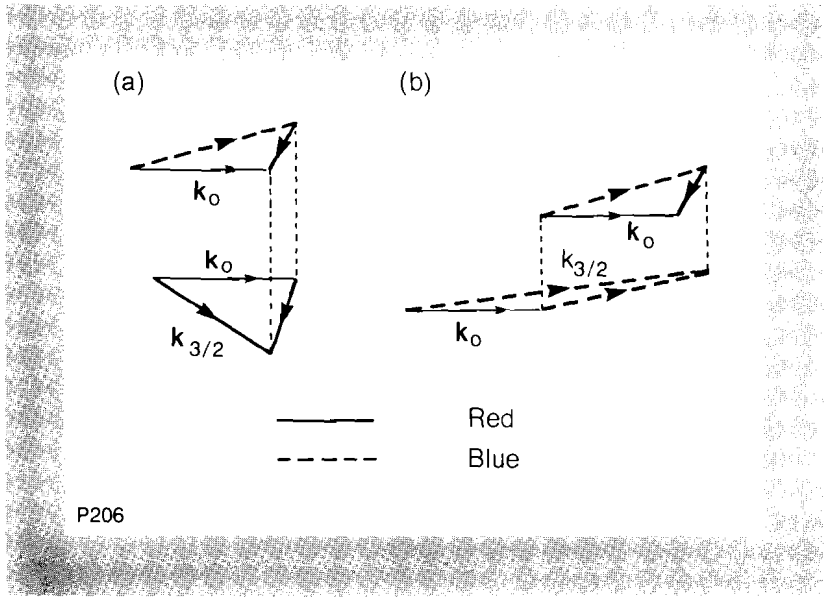

Fig. 13
a) Wave-vector matching diagram for generation of red forward-scattered 3/2-harmonic. The maximum component of $k_{3/2}$ in the forward direction is k_0, and so the red-shifted 3/2-harmonic cannot be generated within a cone of about 20° around the forward direction.
b) Wave-vector matching for the blue-shifted 3/2-harmonic. Generation of this light is limited to angles near the forward direction.

plasma we get a necessary condition that $n_0 > 7/12\ n_c$ for wave vector matching; a sufficient condition for blue $3\omega_0/2$ generation may require even larger n_c. Thus, we see that blue-shifted $3\omega_0/2$ light should be produced only at background densities near critical. From the diagram we also see that blue $3\omega_0/2$ is generated only in directions close to the forward direction; because of this fact and the high background density, the $3\omega_0/2$ will tend to remain confined to the filament. Finally, the blue plasmons which create $3\omega_0/2$ light have small values of κ ($\kappa \sim 1/2$), so the blue shifts should be relatively small.

Figures 14 and 15 show the consequences of this model for overdense and underdense planar target experiments, respectively. In Fig. 14, the overdense case, we see that both red and blue $3\omega_0/2$ light is spread over a wide range of angles, in such a way that the angular dependence of the spectral shifts should be eliminated. In the underdense case (Fig. 15) the red-light angular dependence is also lost, though we expect the forward-scattered light to show a smaller red shift than the backscattered $3\omega_0/2$, and we also expect red light to be excluded from the forward direction. Since the filament can extend through the underdense plasma, the blue light remains confined throughout the filament and emerges in a small cone around the forward direction. Two observations of this forward-scattered light are indicated here, one of which (LLE) at 135° saw only red light, while the other at Livermore, an observation with 1060-nm incident light at ~ 150°, saw only blue light, in accordance with our theory (Sec. 2.D, Ref. 3).

In short, we have shown that the threshold condition for the occurrence of TPD in filaments is readily satisfied. For overdense target experiments, the resulting $3\omega_0/2$ emission spectrum should have two peaks, one shifted to the blue and the other shifted two to three times farther to the red from the exact $3\omega_0/2$ frequency. The splitting should show little dependence on angle of observation. For underdense planar targets, the red peak should have a larger shift in

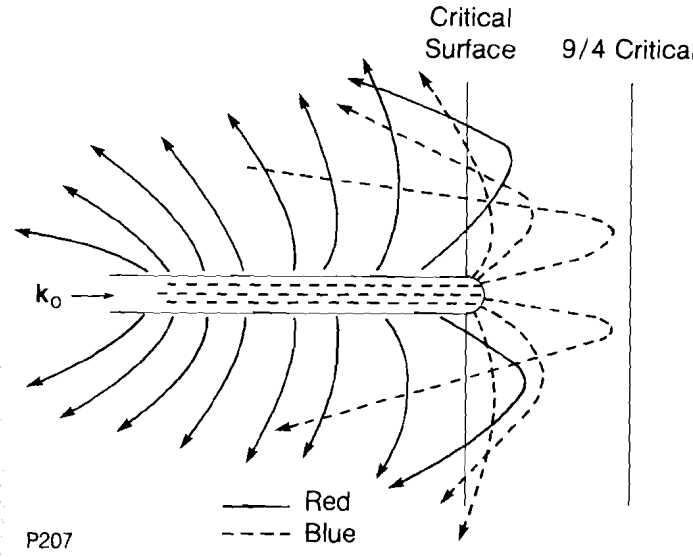

Fig. 14
Generation of 3/2-harmonic by filaments in underdense plasma target. Both red and blue components are scattered widely, so that the angular dependence of the spectral splitting is largely averaged out.

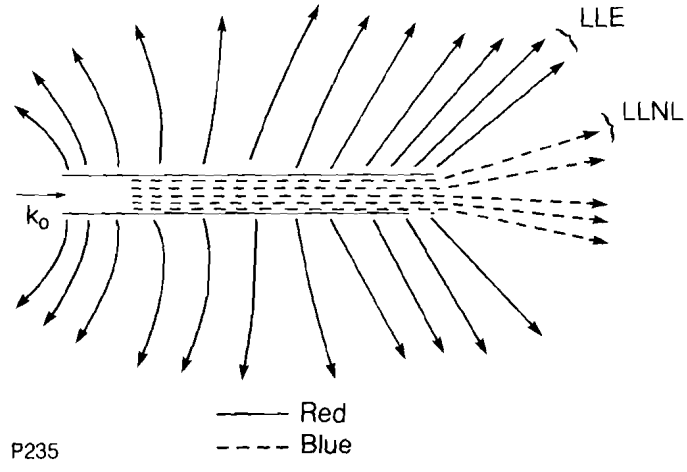

Fig. 15
Generation of 3/2-harmonic by a filament in an underdense planar target. Blue-shifted light is confined to narrow forward cone; red-shifted light is excluded from forward direction. These features of forward-scattered 3/2-harmonic shown are discussed in the text.

backscatter than in forward scatter, and should be excluded from a cone of about 20° around the forward direction. The blue peak should be seen only very near the forward direction. These predictions seem to agree well with experimental observations so far; further experiments are planned to test the theory more thoroughly.

REFERENCES

1. H. A. Baldis and C. J. Walsh, *Phys. Fluids* **26** , 1364 (1983).

2. LLE Review **14** , Section 2.B (1982).

3. C. S. Liu and M. N. Rosenbluth, *Phys. Fluids* **19**, 967 (1976).